Strong and weak adsorptions of polyelectrolyte chains onto oppositely charged spheres

A. G. Cherstvy[a)]
Max-Planck-Institut für Physik komplexer Systeme, Nöthnitzerstrasse 38, D-01187 Dresden, Germany and Institut für Festkörperforschung, Theorie-II, Forschungszentrum Jülich, D-52425 Jülich, Germany

R. G. Winkler
Institut für Festkörperforschung, Theorie-II, Forschungszentrum Jülich, D-52425 Jülich, Germany

(Received 10 April 2006; accepted 23 June 2006; published online 9 August 2006)

We investigate the complexation of long thin polyelectrolyte (PE) chains with oppositely charged spheres. In the limit of strong adsorption, when strongly charged PE chains adapt a definite wrapped conformation on the sphere surface, we analytically solve the linear Poisson-Boltzmann equation and calculate the electrostatic potential and the energy of the complex. We discuss some biological applications of the obtained results. For weak adsorption, when a flexible weakly charged PE chain is localized next to the sphere in solution, we solve the Edwards equation for PE conformations in the Hulthén potential, which is used as an approximation for the screened Debye-Hückel potential of the sphere. We predict the critical conditions for PE adsorption. We find that the critical sphere charge density exhibits a distinctively different dependence on the Debye screening length than for PE adsorption onto a flat surface. We compare our findings with experimental measurements on complexation of various PEs with oppositely charged colloidal particles. We also present some numerical results of the coupled Poisson-Boltzmann and self-consistent field equation for PE adsorption in an assembly of oppositely charged spheres. © *2006 American Institute of Physics*. [DOI: 10.1063/1.2229205]

I. INTRODUCTION

The complexation of a polyelectrolyte (PE) chain with oppositely charged spherical objects has important applications in physics and biology. Nature uses such complexes of DNA with histone proteins as fundamental building blocks for compactification of genetic material in chromatin.[1,2] The complexes of DNA with oppositely charged species are also extensively used *in vitro*, in particular, for the purposes of gene therapy. The electrostatic coupling between the oppositely charged species within a complex influences its structural and dynamic properties. The properties of complexes of spherical macroions with adsorbed PE chains of different lengths and flexibilities have been studied theoretically,[3–13] experimentally,[14–21] and by computer simulations.[22–27] An important aspect of such complexes is overcharging, for which several mechanisms have been proposed and explored.[3,7,11] Still a number of features of complexation, such as critical conditions for PE adsorption, the charge of the complex, the thickness of the polymer layer, etc., are not yet completely understood, neither for the strong nor for the weak adsorption limit.

In the limit of *strong* adsorption (highly charged PEs or low temperatures), when PE adsorption energy to the sphere is large compared to thermal fluctuations of the chain, the adsorbed PE forms well-defined patterns on the sphere surface (rosettes, tennis-ballpattern, solenoids, etc.), which have been predicted theoretically,[3,6,7,25] observed in computer simulations,[22,27] and in experiments.[21] The arrangement of the PE chains on the sphere is dictated to a large extent by maximization of PE-sphere electrostatic attraction and minimization of PE-PE electrostatic repulsion. To determine the interplay between various energies, usually the superposition of the electrostatic potentials is used, because the calculation of the exact solution for the electrostatic potential and energy created by a *nonuniform* charge distribution on the sphere can be complicated. The latter problem has been solved for some charge patterns within the Poisson-Boltzmann theory.[28–30]

In the limit of *weak* adsorption, a crowding of fluctuating PE chains occurs adjacent to the oppositely charged surfaces that may or may not result in PE adsorption. In the limit of zero curvature, the theory of PE adsorption onto planar surfaces has been developed in a number of works,[31–47] including the treatments of nonhomogeneous surface charge distributions.[48,49] The PE adsorption onto charged surfaces that create a screened Coulomb potential has been studied, in particular, on the basis of the Green function approach using the Edwards path integral equation in the ground state dominance approximation.[43,44] These theories predict the existence of critical adsorption conditions for the polymer binding. For curved surfaces such as cylinders and spheres, the PE adsorption has also been studied; although no exact solution of the Edwards equation exists in these cases, some variational approaches have been suggested.[4,46] The properties of PE-surfactant complexes have also been studied for different PE flexibilities. The general tendency is that the critical adsorption temperature is reduced by a positive sur-

[a)]Author to whom correspondence should be addressed. Electronic mail: cherstvy@pks.mpg.de

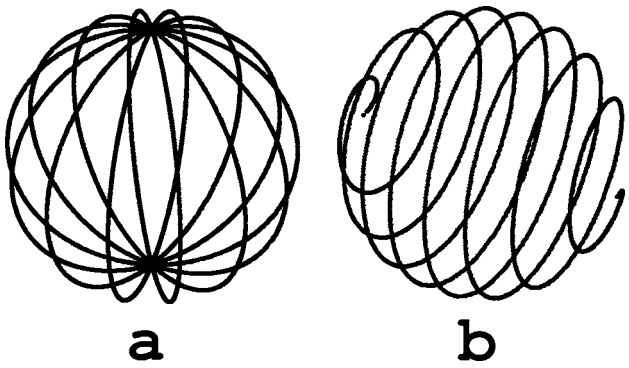

FIG. 1. Two possible wrapping scenarios for a PE chain wrapped around an oppositely charged sphere in the strong adsorption limit. For (a) $N_c=14$.

face curvature, since curved surfaces decrease the number of PE-surface attractive contacts and increase the number of possible chain conformations.[4]

In this paper, we study various scenarios of PE adsorption onto oppositely charged spheres. In Sec. II, we consider the limit of strong PE adsorption. We solve the linear Poisson-Boltzmann equation for nonhomogeneously charged PE-sphere complexes and calculate the electrostatic potential and electrostatic energy of the complex. We calculate the optimal charge of the complex and show that it is always undercharged by wrapped PE. This part is the continuation to spherical geometry of the problem of PE-cylinder complexation considered by the authors in Ref. 50. In Sec. III the limit of weak adsorption is discussed. The Edwards equation for a PE chain near an oppositely charged sphere is solved in some approximate potential (Hulthén potential) that represents the Debye-Hückel sphere potential in electrolyte solution. The conditions of the onset on PE-sphere complexation are analyzed, including their dependence on the Debye screening length and sphere radius. Similar to PE adsorption onto planar surfaces, there exists a critical sphere charge density below which no PE adsorption takes place. In Secs. II C and III C, we discuss the relation of our results to experimental findings.

II. STRONG PE-SPHERE ADSORPTION

We present a calculation of the energy of infinitely thin uniformly charged PE strings wrapped around an oppositely charged sphere of radius a and of uniform surface charge density σ. The chains assume a definite conformation on the sphere surface (cf. Fig. 1). No chain fluctuations (either low temperatures or highly charged or rigid PE chains) and no charge distribution inside the sphere are considered.

A. Basic equations

The electrostatic potential $\psi(\rho,\varphi,\vartheta)$ created by the spherical complex outside[51] the sphere satisfies the linear Poisson-Boltzmann equation

$$\Delta\psi=\kappa^2\psi, \tag{1}$$

where $\kappa=\sqrt{8\pi l_B n_0}$ is the reciprocal Debye screening length of the 1:1 salt solution and Δ is the Laplace operator in spherical coordinates. The charge density of the sphere with the wrapped PE string is

$$\sigma(\rho,\varphi,\vartheta)=\delta(\rho-a)\sigma(\varphi,\vartheta), \tag{2}$$

where $\delta(x)$ is the Dirac delta function. The electrostatic energy of the complex follows from the expression

$$E_{\mathrm{el}}=\frac{a^2}{2}\int_0^{2\pi}d\vartheta\int_0^{\pi}d\vartheta\,\sin\vartheta\psi(a,\varphi,\vartheta)\sigma(\varphi,\vartheta). \tag{3}$$

In the following considerations, we restrict ourselves to the wrapping scenario (a) of Fig. 1. For scenario (b) the calculations are similar but more cumbersome due to a lower symmetry of the problem, see Ref. 52.

We expand the electrostatic potential in terms of the spherical harmonics

$$Y_{lm}(\varphi,\vartheta)=A_{lm}e^{im\varphi}P_l^m(\cos\vartheta) \tag{4}$$

and of spherical Bessel functions,

$$\psi(\rho,\varphi,\vartheta)=\sum_{i=0}^{\infty}\sum_{m=-l}^{l}C_{lm}Y_{lm}(\varphi,\vartheta)\frac{K_{l+1/2}(\kappa\rho)}{\sqrt{\kappa\rho}}. \tag{5}$$

Here $P_l^m(\cos\vartheta)$ are the associated Legendre polynomials and $A_{lm}=\sqrt{(2l+1)(l-m)!/[4\pi(l+m)!]}$. [The radial component of the potential satisfies the equation $\rho^{-2}d(\rho^2dR_l(\rho)/d\rho)/d\rho-[l(l+1)/\rho^2+\kappa^2]R_l(\rho)=0$ and has the solution in the form $R_l(\rho)=A_lI_{l+1/2}(\kappa\rho)/\sqrt{\kappa\rho}+B_lK_{l+1/2}(\kappa\rho)/\sqrt{\kappa\rho}$; for $\kappa=0$ the radial eigenfunctions are ρ^l and $\rho^{-(l+1)}$.] This yields the separation of variables in the Poisson-Boltzmann equation. The coefficients C_{lm} depend on $\sigma(\varphi,\vartheta)$ and can be found from the Gauss theorem applied at $\rho=a$; using the orthogonality of Y_{lm} one finds

$$C_{lm}=-4\pi\varepsilon^{-1}k_l^{-1}\int_0^{\pi}d\vartheta\,\sin\vartheta\int_0^{2\pi}d\vartheta\sigma(\varphi,\vartheta)Y_{lm}^*(\varphi,\vartheta). \tag{6}$$

Here $k_l(a)=[2\kappa aK'_{l+1/2}(\kappa a)-K_{l+1/2}(\kappa a)]/(2a\sqrt{\kappa a})$ [note that $k_l(a)<0$], $K'_{l+1/2}(x)$ is the derivative of $K_{l+1/2}(x)$ and Y_{lm}^* is the complex conjugate of Y_{lm}.

The potential of the *uniformly* charged sphere $\psi_0(\rho)$ with the charge density σ depends on the separation from the sphere ρ only, i.e., only the term with $l=m=0$ survives in Eq. (5). Since $K_{1/2}(\kappa\rho)=\sqrt{\pi/2}e^{-\kappa\rho}/\sqrt{\kappa\rho}$, one obtains the well-known Debye-Hückel expression for the potential

$$\psi_0(\rho)=4\pi a^2\sigma e^{-\kappa(\rho-a)}/[\varepsilon\rho(1+\kappa a)] \tag{7}$$

and

$$E_0=8\pi^2a^3\sigma^2/[\varepsilon(1+\kappa a)] \tag{8}$$

for the sphere electrostatic energy.

B. Results and discussion

For a negatively charged sphere covered by N_c equally spaced positively charged *semicircles*, which cross at the sphere poles like meridians on a globe [cf. Fig. 1(a)], the charge density is given by

$$\sigma(\varphi,\vartheta)=\sigma-2\pi\sigma N_c^{-1}\theta\sum_{s=0}^{N_c-1}\delta\left(\varphi-\frac{2\pi s}{N_c}\right), \tag{9}$$

where the azimuthal angle of sth semicircle is $\varphi=2\pi s/N_c$ (the PE is negatively charged). The ratio of the total charge of adsorbed PE to the sphere charge is θ. The charge density (9) yields the following converging series for the electrostatic potential:

$$\psi(\rho,\varphi,\vartheta)=\psi_0(\rho)(1-\theta)+16\pi^2\sigma\theta\varepsilon^{-1}\sum_{l=0}^{\infty}{\sum_{m=0}^{l}}'\delta_{m,jN_c}A_{lm}^2J_{lm}k_l^{-1}\times P_l^m(\cos\vartheta)\cos[m\varphi]\frac{K_{l+1/2}(\kappa\rho)}{\sqrt{\kappa\rho}} \tag{10}$$

and energy of the complex

$$E_{\mathrm{el}}=E_0(1-\theta)^2-16\pi^3a^2\sigma^2\theta^2\varepsilon^{-1}\sum_{l=0}^{\infty}{\sum_{m=0}^{l}}'\delta_{m,jN_c}A_{l,m}^2J_{lm}^2k_l^{-1}\frac{K_{l+1/2}(\kappa a)}{\sqrt{\kappa a}}. \tag{11}$$

The prime of the second sum indicates that the terms with $m=0$ have to be multiplied by $1/2$ and the term with $m=l=0$ is not counted in the sum because it is included in the uniform part of the potential and the energy, respectively. In the sums only the terms with $m=jN_c$, where j is an integer, survive. The integral in Eq. (6) can be expressed by gamma functions (Γ) and the generalized hypergeometric ($_3F_2$) functions as[53]

$$\begin{aligned}J_{lm}&=\int_{-1}^{1}P_l^m(x)dx\\&=(1+(-1)^{l+m})\pi(-1)^m2^{-2m-1}\Gamma(1+m+l)\\&\quad\times{}_3F_2(\{m/2+l/2+1/2,m/2-l/2,m/2+1\},\\&\quad\{m+1,m/2+3/2\},1)/[\Gamma(1/2+m/2)\\&\quad\times\Gamma(1-m+l)\Gamma(m/2+3/2)].\end{aligned} \tag{12}$$

The electrostatic potential in Eq. (10) is the sum of the bare potential ψ_0 and corrections due to the discreteness of the charge pattern. The dependence of the dimensionless potential $\Psi=e_0\psi/(k_BT)$ on the angles φ and ϑ is depicted in Fig. 2. The magnitude of the potential variation decreases in the regions close to the "poles," i.e., when $\vartheta\to0$. The potential $\Psi(\varphi)$ rapidly decreases as we move away from the sphere and decreases with increasing number of circles, as shown in Fig. 2(b). Note that although Ψ can be larger than unity for large values of $|\sigma|$, we expect our *linear* electrostatic model to grasp the potential variation qualitatively correctly.

Similarly, the energy of the complex consists of two terms. The first term is the energy of the sphere and of the *uniformly smeared* charge of the wrapped PE; this term favors electrically neutral complexes. The positive energy corrections in the sums originate from the electrostatic energy of adsorbed PE circles. These corrections decrease in magnitude when the number of circles increases (provided that the total charge of the wrapped polymer is kept constant). Hence, within this model the adsorbed PE *cannot* overcharge the sphere. This result is similar to that of helically wrapping PEs on an oppositely charged cylinder considered in Ref. 50.

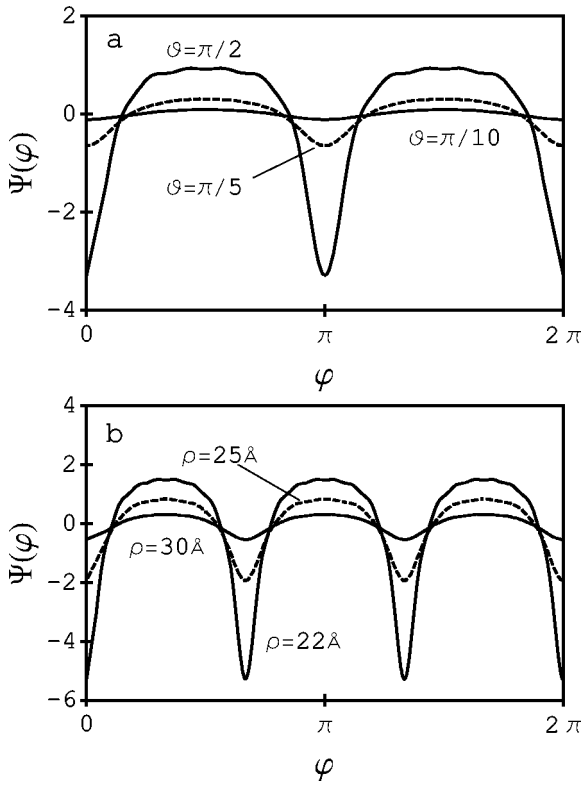

FIG. 2. The "latitude" variation of the electrostatic potential around the spherical complex depicted in Fig. 1(a). Parameters: $a=20$ Å, $\theta=1$, $\sigma=e_0/300$ Å^2, $\kappa^{-1}=7$ Å; (a) $\rho=25$ Å, $N_c=2$, $\vartheta=\pi/2$, $\pi/5$, and $\pi/10$; and (b) $N_c=3$, $\vartheta=\pi/2$, $\rho=22$, 25, and 30 Å.

Let us consider the elastic energy of PE bending. For a *semiflexible* PE with a finite persistence length l_p, the inevitable chain bending upon adsorption onto a sphere disfavors PE wrapping and shifts the equilibrium towards undercharged complexes. We calculate for the scenario of Fig. 1(a) the optimal number of adsorbed PE circles N_c that correspond to the minimum of the electrostatic energy of the complex (11) and PE mechanical bending energy $E_b=k_BTl_p\pi N_c/(2a)$. We take the linear charge density of the wrapped PE to be e_0/b, where b is the PE charge-charge separation. As one could expect, the neutralization fraction of the sphere by the PE,

$$\theta=N_c|e_0/\sigma|/(4ab), \tag{13}$$

decreases as the adsorbed PE becomes stiffer, see Fig. 3. With increasing number of circles the energy corrections due to discreteness decrease in magnitude, i.e., the uniform energy term proportional to $(1-\theta)^2$ dominates, resulting in θ values close to unity. In Fig. 3, the optimal number of wrapped PE circles follow the dependence of $\theta(l_p)$; for parameters of Fig. 3 the maximal values of N_c (at $l_p\to0$) are 13 and 26, respectively, for dashed and solid curves. As N_c is an integer number by definition, a staircase like behavior for optimal θ is observed. At some critical value of l_p the PE

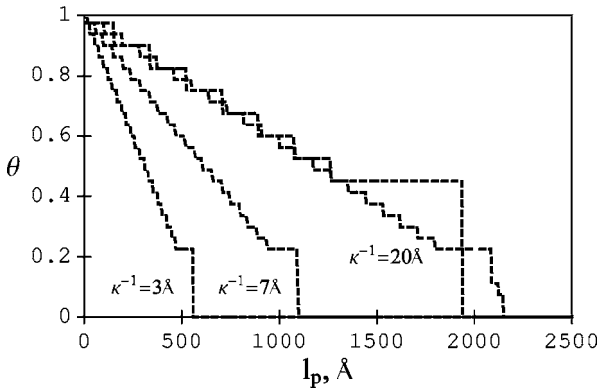

FIG. 3. The dependence of the neutralization fraction for the complex of Fig. 1(a) on the PE persistence length l_p. Parameters: $\sigma=e_0/30$ Å^2, $a=20$ Å; for the dashed curve: $b=5$ Å, $\kappa^{-1}=7$ Å; and for the solid curves: $b=10$ Å and $\kappa^{-1}=3$, 7, and 20 Å.

bending penalty exceeds the energy of PE electrostaticattraction to the sphere, and the value of θ drops abruptly to zero. This corresponds to PE desorption transition.

In general, the adsorption of a PE directly onto a sphere surface occurs only if l_p is smaller than a critical value, namely, when the energy gain upon adsorption exceeds the elastic energy cost of chain bending around the sphere. This condition is based on chain persistence and it results in two simple predictions for the adsorption-desorption equilibrium. For $\kappa a \gg 1$ adsorption occurs for $l_p < 2Zl_B/(b\kappa)$, where $Z=4\pi a^2|\sigma/e_0|$ is the number of the sphere charges. Thus, the sphere charge density scales like $\sigma_c \propto \kappa$ in this regime. In the limit of small κ, one has to account for the electrostatic contribution to the PE persistence length[54] that leads to the inequality $Z_c > 1/(8ab\kappa^2)$, i.e., we get $\sigma_c \propto \kappa^{-2}$. These scaling regimes were obtained in Ref. 25 after numerical minimization of the Debye-Hückel PE-sphere and the PE-PE interactions. Such simple consideration can, however, result in (unrealistically) high degree of sphere overcharging by wrapped PE (for instance, up to ~30 times overcharging for complexes mimicking DNA-histone complexes has been reported in Ref. 25). One of the other ideas of overcharging of weakly charged spheres was suggested in Ref. 3 for the situation when PE chains are in access in the solution.

Also, a strong overcharging of spherical particles covered by adsorbed strongly oppositely charged PEs was predicted by Shklovskii and co-workers, treating the problem by an approach reaching *beyond* the mean-field theory. Their analysis is based on the image-charge attraction of additional PEs to the adsorbing surface and on the picture of a strongly correlated liquid of PEs on the substrate (Wigner crystal).[7(a),45] The charge inversion, driven by repulsive correlations of PEs on the macroion surface, was shown to become more pronounced with increasing salt concentration in the solution; it can reach up to 200%–300% for solenoidlike complexes depicted in Fig. 1(b).[7] Although in our model the pattern of adsorbed PEs also reveals strong correlations, they are treated within the *mean-field* Poisson-Boltzmann theory and thus the *isoelectric* complexes are always favored energetically (in the next subsection see also the discussion of experiments on isoelectric PE complexation). Note also that for PEs of finite thickness an *asymmetric* charge neutralization upon adsorption onto the sphere can result in overcharging of the complex even in the mean-field description that might have a relevance to overcharging of histone proteins by DNA in nucleosome core particles, see Ref. 11.

By using the general expansion (5), the potential and energy for an *arbitrary* static PE charge distribution on the sphere surface can be calculated. However, we neither consider a more complicated situation with, for example partially adsorbed polymers, nor do we compare the complex energy with the energy of the PE and the sphere in their free state in solution. Also, we do not calculate which of the two "zero-temperature" wrapping scenarios of Fig. 1 is favored electrostatically for a given charge density and length of the PE chain.

Other scenarios, such as tennis-ball-like,[7] rosettelike,[6,12] and equator-wrapping[21] structures, are also possible candidates of ordered (Wigner-crystal-like) structures that minimize the electrostatic energy. For all these structures, in the strong adsorption limit, we expect to see nearly neutral or undercharged complexes within our model. At finite temperatures, the chain fluctuations are expected to diminish the amount of adsorbed PEs. Inherently, the adsorption of a neutral fluctuating semiflexible polymer onto a spherical surface is a nontrivial problem,[12,55] and the presence of charges further complicates the behavior of the adsorbed polymer chain. However, we would like to point out that for uncharged polymers with large persistence lengths ($4l_p > a$) the optimal conformation was obtained in Ref. 12 to be similar to that of Fig. 1(a).

C. Experiments on PE wrapping and interaction of complexes: DNA and nucleosome

The wrapping scenarios on Fig. 1 considered above can mimic some properties of *DNA-histone complexes* in the nucleosome core particles (NCP), although many important details are neglected in the present analysis. However, the exact calculation of electrostatic interactions within (as well as between) the NCPs—if realistic charge pattern on the DNA, on the basic histone proteins, as well as on the highly charged histone tails are considered—is a complicated task (which is likely to be solvable numerically only).

Our results can also be applied to complexation of DNA with man-made colloidal oppositely charged nanoparticles, reminiscent of DNA-histone complexation in chromatin. For instance, DNA complexed with silica polylysine-coated nanospheres of charge density $\sim e_0/\text{nm}^2$ and with a diameter of 10–100 nm has been studied recently in Ref. 21. DNA was shown to wrap around the nanoparticle making from a couple to about 40 turns (depending on the sphere size and charge density): for a small number of turns the DNA is wrapped on the sphere equator, where the curvature is the smallest. The formation of large aggregates of DNA-nanoparticle complexes with 5–50 spheres per T4-phage DNA was then detected.[21] As the nanoparticle concentration in solution increases, the aggregate becomes more and more compact. In the fully compacted state, the ratio between the total charge of nanoparticles to DNA charge depends on particle size. The aggregates of small nanoparticles are

strongly *undercharged* by wrapped DNA, whereas for the largest nanospheres at intermediate ionic strengths a small *overcharging* of the aggregates has been detected. The compaction was shown to be maximal at nearly physiological ionic strength, reminiscent of DNA-histone complexation in nucleosomes:[56] for $n_0 > 1.5M$, when the electrostatics is well screened, no DNA-nanospheres compaction could be achieved, whereas for small n_0, when the electrostatic contribution to the DNA persistence length grows, the compactification is suppressed. One can suggest that the overcharging (possibly) observed in Ref. 21 for largest particles studied should decrease if enough nanoparticles will be provided in solution to neutralize DNA charge and large equilibrium aggregates will be formed. Note that typically electroneutral aggregates are also observed in other dense self-assembled DNA nanostructures e.g., DNA sandwichlike lamella complexes with cationic lipids,[57] where complexation was suggested to be driven by the release of condensed counterions of DNA and of lipid head groups.

Let us discuss some aspects of electrostatic *interaction* of the studied spherical complexes. In general, for arbitrary PE wrapping pattern and for arbitrary orientations of the complexes in space, this is a complicated mathematical problem. One can suggest that the modulations of the electrostatic potential emerging in solution near the complexes due to the nonhomogeneous charge distributions (see Fig. 1) modify DLVO-like pure repulsion between effective likely charged spheres. Correlation-induced *electrostatic attraction* between the complexes can occur when these potential modulations on the complexes are *in phase*: the potential patches of different sign face each other near the contact of the two complexes, forming an electrostatic zipper. The effective screening length of this electrostatic attraction, $\sim 1/\sqrt{\kappa^2+(2\pi/P)^2}$, is a combination of κ and of a typical period P of alternating positive-negative patches on the surfaces. It is shorter than the decay length of repulsive interactions between uniformly charged spheres, $1/\kappa$. Thus, in order to overcome the net charge repulsion, the complexes should be neutralized to a large extent by the adsorbed PEs (θ should be close to 1) and have to be separated by surface-to-surface distances $\lesssim P$.

Note that such zipperlike electrostatic attraction can be one of the reasons for condensation of DNA molecules,[58,59] and of nucleosome core particles[60,61] in solutions in the presence of some multivalent counterions (see Refs. 59 and 62 for the theory of DNA-DNA electrostatic interaction when the molecules are considered as charged spirals mimicking DNA phosphates and adsorbed cations in the grooves). Such correlation-induced attractive interactions between PE complexes, which consist of PE chains wrapped about two times around oppositely charged spherical colloid, have been reported recently in Ref. 63 at intermediate salt concentrations on the basis of numerical computation. It was suggested that this attraction has a relevance to the internucleosomal attraction observed experimentally at similar ionic conditions.[64] In these experiments, the second virial coefficient of solution of NCPs has been shown to become negative when the concentration of salt becomes larger than ~50 mM for NCP_{145} and larger than ~150 mM for NCP_{165} (the latter has 40 additional DNA phosphate charges). Note, however, that the hypothesis of histone-tails-included NCP-NCP bridging interactions, which will be discussed in Sec. III B, cannot be completely ruled out as an explanation of NCP-NCP attraction (see also Ref. 60).

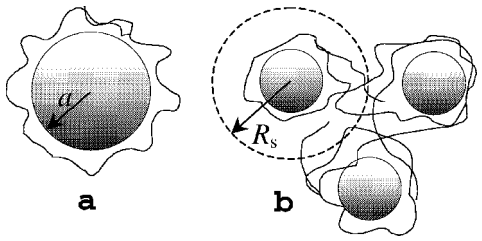

FIG. 4. Weak adsorption limit: (a) crowding of PE around the oppositely charged sphere and (b) PE-induced bridging in an assembly of spheres in the spherical cell model.

III. WEAK PE-SPHERE ADSORPTION

A. Edwards equation and Hulthén potential

In this section, we consider the weak adsorption of flexible fluctuating PEs onto an oppositely charged sphere [see Fig. 4(a)] within a self-consistent field approximation. The PE is considered to be weakly charged in this limit and Gaussian statistics of its fluctuations is assumed to be only slightly perturbed by electrostatic interactions with the sphere. In general, upon polymer adsorption onto surfaces with a positive curvature, the polymer configurations are less perturbed as compared to adsorption onto a flat surface. On the other hand, the contact area with the attractive surface is decreased by the positive curvature.

The polymer distribution near the sphere as well as the critical adsorption conditions for PE adsorption have been calculated on the basis of the variational approach in Ref. 4 using the Edwards equation in the ground state dominance approximation. We adopt the same polymer model and also exploit the Edwards equation. In particular, we do not take into account both PE-PE electrostatic (see Ref. 65) and PE excluded volume interactions explicitly; both contributions can be captured via an effective Kuhn length, as it was suggested in Ref. 4.

The PE-sphere interaction is given by the Debye-Hückel potential (7). Unfortunately, no analytical solution of the Edwards equation for this potential has been found so far. In order to arrive at an analytical solution of the adsorption-desorption transition, we approximate the sphere potential $\psi_0(\rho)$ by the *Hulthén* potential,[5,66]

$$\psi_H(\rho) = \frac{4\pi a\sigma(e^{\kappa a}-1)}{\varepsilon(1+\kappa a)}\frac{e^{-\kappa\rho}}{1-e^{-\kappa\rho}}. \tag{14}$$

This approximation works well close to the sphere surface (Fig. 5). Moreover, the difference between the two potentials is small for $\kappa a \gg 1$, since ρ in the denominator is slowly varying and can be replaced by a and $e^{-\kappa\rho} \ll 1$. Using the properties of the bound states of the Edwards equation, we analyze the critical conditions for PE adsorption onto the sphere.

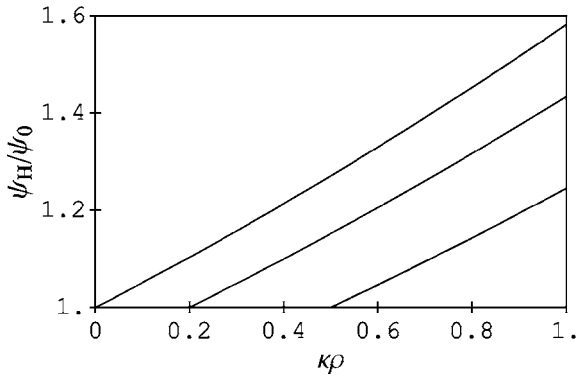

FIG. 5. The ratio of the Hulthén potential and the Debye-Hückel potential as a function of $\kappa\rho$ for $\kappa a=0$, 0.2, and 0.5 (from left to right).

We expand Green's function of a PE chain of length L in terms of eigenfunctions $\phi_n(\rho)$ (Refs. 4, 31, and 44) and the spherical harmonics Y_{lm}

$$G(\rho,\varphi,\vartheta;N|\rho',\varphi',\vartheta';0)=\sum_{n,l,m}\phi_n(\rho)\phi_n^*(\rho')Y_{lm}(\varphi,\vartheta)\times Y_{lm}^*(\varphi',\vartheta')e^{-\lambda_{nlm}L}. \quad (15)$$

For a spherically symmetric potential in the ground state approximation, i.e., $n=l=m=0$, ϕ_0 obeys the equation[4,5]

$$-\frac{b}{6}\frac{d^2(\rho\phi_0(\rho))}{\rho d\rho^2}-\frac{4\pi a|\sigma\varrho|(e^{\kappa a}-1)}{\varepsilon k_BT(1+\kappa a)}\frac{e^{-\kappa\rho}}{1-e^{-\kappa\rho}}\phi_0(\rho)=\lambda_0\phi_0(\rho), \quad (16)$$

where b is the Kuhn length and ϱ is the PE linear charge density (not to be mixed with ρ). Below, no counterion condensation on PEs is taken into account for the calculation of the real value of ϱ. As $a\to\infty$ the sphere potential turns into the potential of a planar surface and Eq. (16) describes the PE adsorption onto a flat surface studied in Ref. 43. The eigenvalue λ_0 has to be determined from the boundary conditions $\phi_0(a)=\phi_0(\infty)=0$.

By introducing dimensionless variables according to $x=\kappa\rho$, Eq. (16) turns into

$$\frac{1}{2}\frac{d^2\chi_0(x)}{dx^2}+\frac{1}{\delta}\frac{e^{-x}}{1-e^{-x}}\chi_0(x)=a_0^2\chi_0(x) \quad (17)$$

for the function $\chi_0(x)=x\phi_0(x)/\kappa$, the eigenvalue $\lambda_0=-b\kappa^2a_0^2/6$, and with

$$\delta=\frac{\kappa^2b\varepsilon k_BT}{12\pi a|\sigma\varrho|}\frac{1+\kappa a}{e^{\kappa a}-1}. \quad (18)$$

Now a_0 is determined from the boundary conditions. After the substitution $\chi_0(x)=e^{-a_0x}\Phi_0(x)$ and change of the variable to $y=1-e^{-x}$,[66] the eigenfunction equation turns into the hypergeometric differential equation

$$y(1-y)\frac{d^2\Phi_0(y)}{dy^2}-y(1+2a_0)\frac{d\Phi_0(y)}{dy}+\frac{2}{\delta}\Phi_0(y)=0. \quad (19)$$

The solution, which satisfies the boundary condition for $\rho\to\infty$, is

$$\Phi(y)=yF(\alpha,\beta,\alpha+\beta-1;1-y), \quad (20)$$

where $\alpha=a_0+1-\sqrt{2/\delta+a_0^2}$, $\beta=a_0+1+\sqrt{2/\delta+a_0^2}$, and $F(\alpha,\beta,\gamma;y)$ is the Gaussian hypergeometric function ${}_2F_1$.[67] The adsorption transition occurs for $\lambda_0=0$, i.e., when λ_0 switches from positive to negative values. Hence, the parameter δ assumes a particular value δ_c for a given κa, which is determined from the condition of zero PE concentration on the sphere surface

$$F(1-\sqrt{2/\delta_c},1+\sqrt{2/\delta_c},1;e^{-\kappa a})=0. \quad (21)$$

For $\kappa a\ll 1$, the critical δ follows from the condition

$$\delta_c\lesssim 2, \quad (22)$$

which yields the critical adsorption temperature T_c.

Our model predicts that no adsorption occurs on the sphere at $T>T_c$. The eigenfunction ϕ_0 decays like $\phi_0\sim(1-e^{-x})/x$ for large x, because the hypergeometric function approaches the limiting value $F=1$. In general, δ_c decreases as a function of κa starting from $\delta=2$ for small κa. For large κa, δ_c decays exponentially as $\delta_c=(8/j_0)^2e^{-\kappa a}$, where j_0 is the first positive root of the Bessel function of the first kind, J_0. A more detailed discussion is presented in Ref. 5. For parameters of the system where $\delta<\delta_c$, PE adsorption takes place and the PE concentration is a function of a_0.

Using the definition of δ (18) and the critical condition (22), we find that for the spheres with $\kappa a\ll 1$ the critical adsorption temperature is

$$k_BT_c\approx 24\pi|\sigma\varrho|a^2/(\varepsilon\kappa b). \quad (23)$$

This condition couples the sphere and PE charge densities, the screening length of the solution, and temperature. The critical temperature is proportional to σ, and T_c decays as $1/\kappa$. That is, as attractive PE-sphere interactions become more screened, the chains remain free at lower temperatures. The critical temperature predicted from the variational approach in Ref. 4 is

$$k_BT_c^M=24\pi|\sigma\varrho|a/(\varepsilon\kappa^2b) \quad (24)$$

in the limit of small κa, i.e., it exhibits a quadratic dependence on the screening length. For PE adsorption onto a planar surface, i.e., $\kappa a\to\infty$, with the same charge density σ, the critical adsorption temperature is[43,44]

$$k_BT_c^W=96\pi|\sigma\varrho|/(j_0^2\varepsilon\kappa^3b), \quad (25)$$

i.e., it reveals even stronger dependence on κ.

The solution of Eq. (21) shows that the exponent of κ increases monotonically from unity at small κa to the third power in κ for large κa, see Fig. 6 and also Ref. 5. As we will show below, the linear dependence of the critical sphere charge density σ_c on κ, predicted by our model for small κa, is closer to a number of experimental observations on complexation of various PEs with oppositely charged spherical particles (see Sec. III C) than the dependence $\sigma_c\propto\kappa^3$ obtained for the PE adsorption onto a planar surface [Eq. (25)]. Hence, by using the Hulthén potential, we have described PE adsorption onto a sphere for *all* radii, including the correct transition to the planar case.

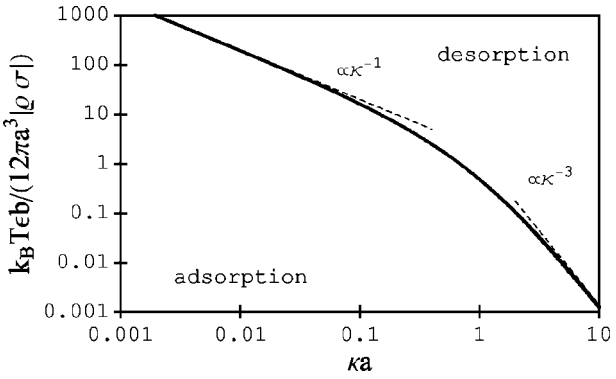

FIG. 6. The critical adsorption temperature as a function of κa as obtained from the analysis of Eq. (19).

The segments of the PE molecule which are in close proximity to the sphere surface effectively renormalize its charge. Hence, the surface charge seen by chain monomers far apart from the sphere is smaller than that for the monomers that are close to the surface. Eventually, upon PE aggregation onto the sphere the effective sphere charge density can become smaller than σ_c, which prevents the overcharging of the complex. This is similar to the conclusion of the previous section for the strong adsorption limit. Note that if a low-dielectric sphere core would exist, it would lead to a depletion of PE monomers close to the sphere[9] and thus effectively decrease the value of T_c.

We will now analyze the thickness of the PE adsorbed layer near an oppositely charged plane and around an oppositely charged sphere. For the plane, the ground state solution corresponds to the maximum value $\bar{\nu}$, which is found from the equation[43]

$$J_{\bar{\nu}}(\sqrt{96\pi|\sigma\varrho|/(\varepsilon k_B T b\kappa^3)}) = 0. \tag{26}$$

The first solution with $\bar{\nu}=0$ yields $\sqrt{96\pi|\sigma\varrho|/(\varepsilon k_B T b\kappa^3)} = j_{0,1}$. This corresponds to the adsorption-desorption transition and leads to Eq. (25) for the critical adsorption characteristics. At larger values of the argument several solutions of Eq. (26) may exist, which then describe the excited states. When the argument of the Bessel functions is larger than $j_{0,1}$, the order $\bar{\nu}$ also increases (see Fig. 7). In the ground state, the width w of the PE density distribution as measured at 1/2 of the height is $\propto J_{\bar{\nu}}(\sqrt{96\pi|\sigma\varrho|/(\varepsilon k_B T b\kappa^3)}e^{-\kappa s/2})^2$, where s is the separation from the plane, and it decreases as the plane

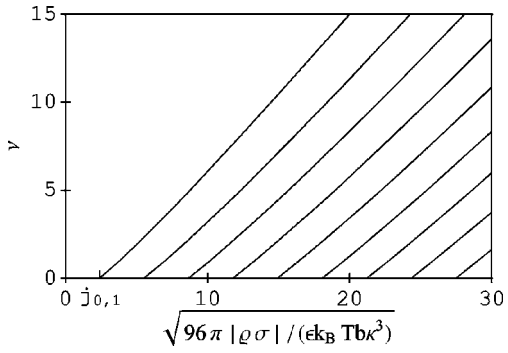

FIG. 7. The order of the Bessel functions describing the ground and excited states of the PE onto an oppositely charged planar surface, see Ref. 43.

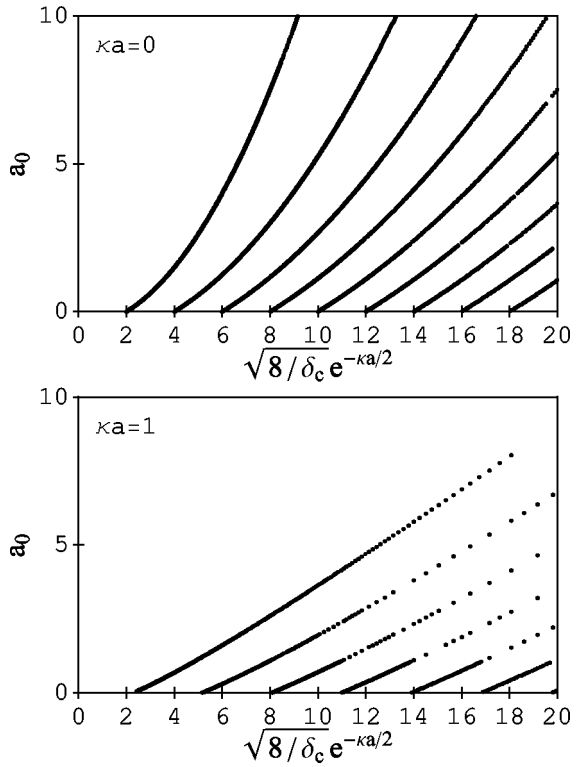

FIG. 8. The dependence of a_0 on δ_c following from Eq. (27).

charge density σ increases. Close to the critical adsorption point, the width of the layer diverges, whereas far from this point, the scaling relation of $w \propto \sigma^{\approx -0.4}$ is observed (Fig. 9). The width of the PE layer grows with increasing ionic strength of solution and the width diverges as κ approaches the critical value, above which no PE adsorption takes place anymore, similar to PE adsorption onto a planar surface.

For the sphere, to obtain the solutions for δ at nonzero a_0 we numerically solve the equation

$$F(a_0+1-\sqrt{2/\delta+a_0^2}, a_0+1+\sqrt{2/\delta+a_0^2}, 2a_0+1; e^{-\kappa a}) = 0. \tag{27}$$

At small δ there are multiple solutions. Similar to the planar case, for a given value of δ, the solution with the smallest eigenvalue $\lambda=-a_0^2\kappa^2 b/6$, i.e., with the maximum value for a_0, corresponds to the ground state of the system. Figure 8 displays a_0 as a function of $\sqrt{8/\delta}e^{-\kappa a/2}$—the latter turns into $\sqrt{96\pi|\sigma\varrho|/(\varepsilon k_B T b\kappa^3)}$ in the limit $\kappa a \to \infty$—for two different values of κa.

In addition, we calculate the thickness of the adsorbed PE layer—using the value of δ—as a function of system parameters [Eq. (18)]. Similar to the planar situation, the adsorbed PE layer becomes more compact with increase of $|\sigma|$. We find that the adsorption layer for a sphere with $\kappa a \sim 1$ is of comparable thickness to that of the planar surface with the same σ, whereas spheres with small κa exhibit more extended PE layers (Fig. 9). Small spheres require larger σ values for PE adsorption to take place. As σ grows at a fixed value of sphere radius, the value of δ decreases and thus the value of a_0 grows. We observe that as σ decreases the position of the peak of PE density distribution from the sphere

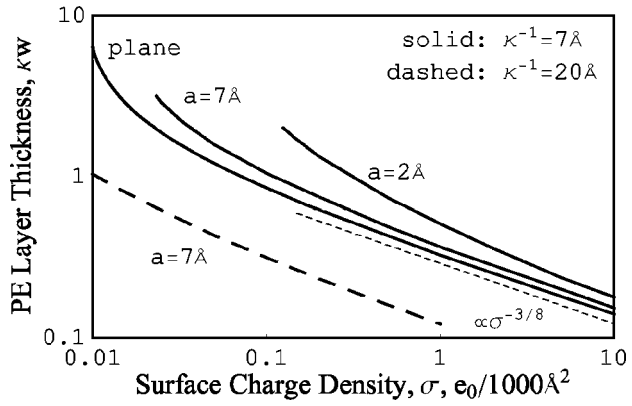

FIG. 9. The thickness of PE density distribution for different sphere radii and screening lengths at $b=1$ Å.

surface does not change considerably, whereas the thickness of the adsorbed layer increases dramatically because of a long tail of the distribution function $\phi^2(r)$.

It was suggested that PEs get trapped in the vicinity of a sphere when the attraction energy of a PE monomer exceeds the penalty of its entropic confinement in the region close to the sphere, $\sim k_BT$.[14,16] This region of high potential around the sphere (the region of a strong PE binding) should become thinner as κ increases (electrostatic potential decays faster away from the sphere) and this region becomes *larger* with increasing sphere charge density. Thus, larger $|\sigma|$ values would be required to form PE-sphere complexes at higher salt concentrations, although this intuitive argument does not give an explanation why the $\sigma(\kappa)$ dependence should be linear as it is observed in many experimentally studied systems.[14,16] Our model, however, predicts that the thickness of PE adsorbed layer increases at larger salt concentration and the PE layer becomes *more compact* with increasing $|\sigma|$.

B. Generalized mean-field theory

In this section we consider a generalization of the self-consistent field approach presented above for a weak adsorption of PEs onto a sphere that includes a *coupling* to the polymer concentration field $\phi^2(\rho)$ and electrostatic potential $\Psi(\rho)$. Our approach is based on the Poisson-Boltzmann equation for the distribution of mobile ions and polymer monomers, which is coupled to the self-consistent field equation in the ground state dominance approximation for polymer distribution.[37] The model neglects any correlations, counterion condensation, and PE stiffening; the PE is treated as a Gaussian chain.

We consider an aggregate of charged spheres in the presence of oppositely charged PE chains. In spherical geometry one can write

$$\frac{\partial^2\Psi(\rho)}{\partial\rho^2}+\frac{2}{\rho}\frac{\partial\Psi(\rho)}{\partial\rho}=\kappa^2\sinh\Psi(\rho)-4\pi l_B p(\phi(\rho)^2-\phi_0^2 e^{\Psi(\rho)}),$$
$$\frac{b}{6}\left(\frac{\partial^2\phi(\rho)}{\partial\rho^2}+\frac{2}{\rho}\frac{\partial\phi(\rho)}{\partial\rho}\right)=v\,\phi(\rho)(\phi(\rho)^2-\phi_0^2)+p\,\phi(\rho)\Psi(\rho). \quad (28)$$

Here, p is the fractional monomer charge, $v\approx b^3$ is the excluded volume parameter, and ϕ_0^2 is the bulk PE concentration (not to be mixed with the eigenfunctions from the previous subsection). These equations have been studied in a number of theoretical works[13,34–37] and have been applied to flexible PEs confined between oppositely charged planar surfaces,[35–37] as well as to aggregates of PEs with oppositely charged spherical particles.[13]

Typically, the PE chains are crowded around localized oppositely charged spheres. When two such spheres are positioned at intermediate separations, the attractive contribution generated by the *overlap of PE clouds* can overcome the net sphere-sphere electrostatic repulsion, giving rise to a negative pressure in the system.[37] At small surface-to-surface separation, the polymer is excluded from the region between the spheres and the latter repel each other. At large sphere-to-sphere distances, PE adsorption occurs on each sphere individually; there is no polyelectrolyte bridging and no attraction. PE adsorption is weaker and a weaker attraction is generated at higher κ and at smaller PE linear charge densities.[37,42]

We use the *spherical cell model* to study the attraction in an assembly of spheres with flexible oppositely charged PEs in the presence of salt [Fig. 4(b)]. We solve Eqs. (28) numerically with the following boundary conditions: on the sphere surface $\partial\Psi(\rho)/\partial\rho|_{\rho=a}=4\pi|\sigma\varrho|/\varepsilon k_BTb>0$ and $\partial\phi(\rho)/\partial\rho|_{\rho=a}=0$; and on the cell boundary $\partial\Psi(\rho)/\partial\rho|_{\rho=R_s}=0$ and $\partial\phi(\rho)/\partial\rho|_{\rho=R_s}=0$. We start solving the equations from the sphere surface and choose the starting value of the electrostatic potential and the polymer concentration such that the boundary conditions on the cell boundary are satisfied. We obtain that the electrostatic potential can be positive on the cell boundary, see Fig. 10. Similar results were obtained for the planar geometry in Ref. 37. Integration of the profiles of mobile ions and PE monomers over the cell results in complete neutralization of the sphere charge, as one

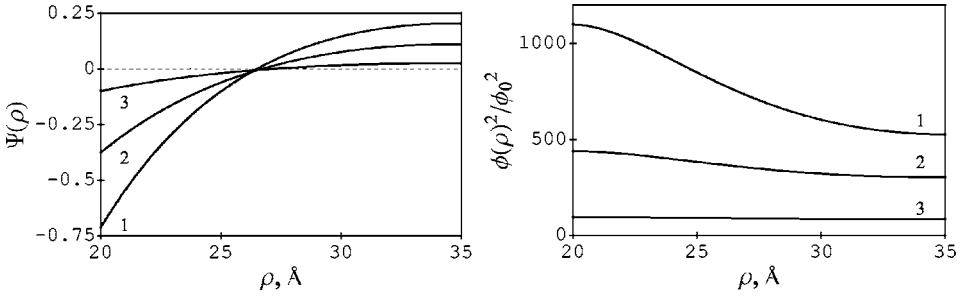

FIG. 10. The variation of electrostatic potential and PE monomer density within the unit spherical cell. Parameters: $b=5$ Å, $p=0.1$, $a=20$ Å, $R_s=35$ Å, $\phi_0^2=10^{-6}$/Å^3, and σ: (1) e_0/500 Å^2, (2) e_0/1000 Å^2, and (3) e_0/4000 Å^2.

could expect. Here we solve Eqs. (28) for $v=0$ and use the condition that $\partial\phi(\rho)/\partial\rho|_{\rho=a}=0$; for real polymers with excluded volume interactions, one has to apply rather the condition of zero PE concentration at $\rho=a$.

The pressure in the cell model can be expressed by the free energy at the cell boundary.[37] This pressure contains the pressure of the neutral polymer, $-k_BTv(\phi(R_s)^2-\phi_0^2)^2/2$; the attractive electrostatic polymer-bridging pressure, $-k_BTp\Psi(R_s)\phi(R_s)^2$; and the repulsive osmotic pressure of the mobile salt ions, $2n_0k_BT[\cosh\Psi(R_s)-1]$, where n_0 is the ion density. The attraction in the system is governed by the interplay of the last two terms and it typically occurs when the electrostatic potentials on the sphere surface and on the cell boundary have opposite signs. Typically, the attraction increases with increasing σ, while for a fixed σ, it increases with decreasing n_0. These findings are in agreement with Figs. 10 and 14 of Ref. 37 obtained for planar surfaces. We observe that at larger cell radii R_s the PE-induced attraction is typically weaker. Also, for large R_s as well as for large n_0, the solutions of (28) become quite sensitive to the boundary conditions we impose on the sphere surface. The typical profiles of electrostatic potential and PE monomer density when the total pressure in the system is attractive are presented in Fig. 10. The detailed analysis of the solutions of (28) as well as the attraction-repulsion behavior in the assembly of spheres with the oppositely charged PEs are beyond the scope of the present paper and will be considered elsewhere.

C. Experiments on PE-micelle complexation

The complex formation between flexible and semiflexible, both biological and synthetic, PEs with oppositely charged spherical colloidal particles, cationic/nonionic micelles, and dendrimers has been systematically studied experimentally by Dubin and co-workers.[16–18] The cationic micelles possess a quite homogeneously charged surface with a charge density σ, which can be tuned continuously by addition of charged and uncharged groups up to several e_0 per 1000 Å^2 (e_0 is the proton charge). Typically, the sphere diameter is ≈20–40 Å, however, considerably larger particles have also been studied. The PE persistence length l_p is of the order of the sphere radius or smaller [≈30 Å for NaPSS, AMPS/AAm copolymers, and PDADMAC; ≈40 Å for hyaluronic acid (HA); and ≈12 Å for PAA];[15,18] more flexible and more rigid PEs have been considered. The considered PEs were in the intermediate charge density regime, typically below the threshold for the Manning counterion condensation,[68] i.e., $\xi<1$.

Experiments have shown that no PE-micelle complexation occurs when the micelle surface charge density is below the *critical* charge density $|\sigma_c|$. Above this density the turbidimetric titration curves reveal a dramatic increase in turbidity that indicates complexation, because the average molecular mass of the complexes is much larger than that of PE alone. The complexes may consist of many PE chains and many colloidal spheres. Total charge close to zero of this PE-colloidal assembly is a necessary condition for higher-order aggregation and phase separation in PE-colloidal mixture. The critical density was shown to be nearly independent of PE molecular weight and PE concentration in solution. It was observed that, as the salt concentration in solution increases, the value of σ_c grows and scales for spherical colloidal particles as[14–16]

$$\sigma_c \propto \kappa^{\nu} \quad \text{with } \nu = 1-1.8. \tag{29}$$

The exponent ν was shown to depend also on the PE linear charge density ξ and on the PE stiffness,[15] which make it a nonuniversal characteristic for the used PEs. Typically, PEs with smaller ξ reveal a stronger dependence of σ_c on κ. The PE-sphere binding affinity was shown to decrease with PE persistence length and to increase with PE linear charge density. Note that for complexation of PEs with different ξ with the spherical dimethyl dodecylamine oxide (DMDAO) micelles a modified dependence for the critical micelle charge density has been suggested, $\sigma_c \propto \kappa^{1.8}\xi^{-0.6}$.[14]

The size of some micelles (DMDAO, for instance) as well as their shape can change with κ: at large salt content, rather cylindrical than spherical micelle shapes are observed. For cylindrical micelles, usually larger scaling exponents have been measured [from $\nu\approx1.4$ for PVAS-DMDAO to $\nu\approx2.5$ for P(AMPS/AAm)-DMDAO complexes.[14]] The DMDAO micelles form complexes also with quite persistent PEs such as double-stranded DNA, providing the exponent $\nu\approx1.6$.[17] Moreover, although the micelle surface charge density is proportional to the micelle protonation degree, which is controlled in experiments via changing the *p*H value, the exact relation for every micelle type is not known. The surface charge density has therefore been obtained for some systems from the *p*H titration data via calculation of the surface potential of the micelle by using the Debye-Hückel solution (7) on the sphere surface.

Experimental values of $\sigma_c(\kappa)$ extracted from several studies on PE-sphere complexation performed by Dubin and co-workers are presented in Fig. 11. In this figure, the Kuhn length for every PE was set to the separation between the nearest PE charges and no dependence of this length on κ was taken into account. We did this purposely because the persistence length l_p has not been measured under the same experimental conditions for all the PEs analyzed and, in addition, the l_p can change in a different manner with the amount of salt in solution for every PE considered. One can see that the values of σ_c observed in experiments are very different for the PEs considered in this figure. Naturally, the presented values of σ_c are higher than those theoretically predicted, simply because the charge separation is usually much smaller than the Kuhn segment length. This particularly applies to the double-stranded DNA: when we set the Kuhn length equal to the DNA persistence length of 50 nm, the experimental data for DNA are very close to the theoretical prediction.

One can see that the slope of experimental curves is 1–1.5 smaller than the theoretical prediction, which in the considered region of κa is already quite close to $\sigma_c \propto \kappa^3$. However, the electrostatic part of the PE persistence length decreases with κ, the scaling relation $l_p^{\mathrm{el}} \propto \kappa^{-1}$ is observed experimentally for some PEs [polyacrylamides P(AMPS/AAm)].[72] Theoretical calculations[44] and computer simulations[69–71] predict $l_p^{\mathrm{el}} \propto \kappa^{-4/5}-\kappa^{-6/5}$, whereas the Odijk-

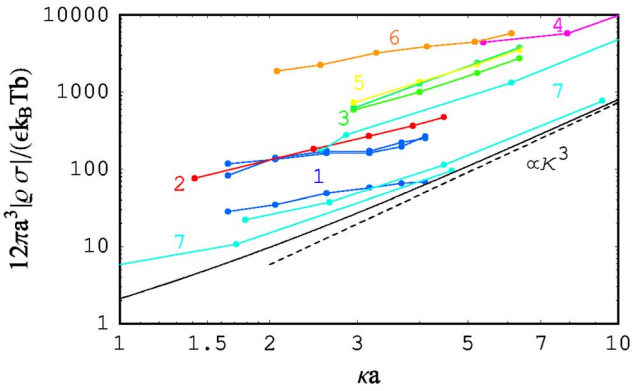

FIG. 11. The dependence of the critical sphere charge density on the screening parameter κa for the complexation of various PEs with oppositely charged spherical colloidal particles. Colors and parameters: dark-blue curves (1) are for PVAS-DMDAO complexation (Ref. 14) with $\nu \approx 1$ (lower curve $b=10$ Å, middle curve $b=4.43$ Å, and upper curve $b=3.18$ Å); red curve (2) is for PDADMAC-CAE/$C_{12}E_6$ (Ref. 18) with $b=6.5$ Å, $\nu \approx 1.4$; green curves (3) are for PAMPS-DMDAO (Ref. 16) with $b=2.55$ Å, $\nu \approx 1$ (upper curve: σ_c is calculated from micelle degree of protonation data; lower curve: σ_c is obtained from the Gouy-Chapman equation); magenta curve (4) is for PDMDAAC-SDS/$C_{12}E_6$ (Ref. 16) with $b=3$ Å, $\nu \approx 1$; yellow curve (5) is for NaPSS-DMDAO (Ref. 18) with $b=2.38$ Å, $\nu \approx 1.4$; brown curve (6) is for DNA-DMDAO (Ref. 17) with $\nu \approx 1.6$, $b=1.7$ Å; and blue curves (7) are for AMPS/AAm-DMDAO (Ref. 14) with $\nu \approx 1.8$ (lower curve: AMPS10/AAm90-DMDAO with $b=25.5$ Å, middle curve: AMPS25/AAm75-DMDAO with $b=10.2$ Å, and upper curve: AMPS50/AAm50-DMDAO with $b=5.1$ Å).

Skolnick-Fixman correction in near-the-rod limit scales[54] like $\propto \xi^2 \kappa^{-2}$ (see also Ref. 73, where the κ^{-2} dependence of l_p^{el} has been reexamined in detail theoretically). This salt-dependent renormalization of the l_p can *decrease* the slope of the $\sigma_c(\kappa)$ predicted theoretically (see Fig. 11) at high salt concentrations, thus providing slopes closer to those observed experimentally of about 1–1.8. The absolute values of σ_c will also be renormalized after using real PE persistence lengths and, if our model is relevant to the underlying physics of the problem, the experimental curves should tend then to follow a single curve. We do not pretend here, however, on a quantitative comparison with the experimental data because our model of a single sphere complexed by a flexible PE is too simple for these purposes and it neglects some important structural features of colloids and PEs. Instead, the complexation of semiflexible PEs with the spheres needs to be considered, which is, however, a separate complicated problem and is beyond the scope of this paper.

Complex formation of PEs with some globular proteins (serum albumin, lysozyme) which possess quite nonhomogeneous charge distributions has also been studied in experiments.[74–76] Some additional interesting effects were detected. For instance, it was shown that PE-protein binding can occur on the *wrong* side of the isoelectric point; also, the negatively charged PEs were shown to bind to *net* negatively charged proteins due to PE electrostatic attraction to *charge patches* on the protein surface.[74] In some cases, the strength of PE-protein binding was shown to have a maximum or a plateau at $\sim 10-30$ mM of simple salt in solution. It was suggested that the corresponding Debye screening lengths are on the order of protein size or of the typical separation of negatively and positively charged domains on the protein surface. Then, at such values of κ the electrostatic attraction of PEs to positively charged protein domains is substantial, whereas the PE repulsion from negatively charged regions is already screened.[75] Further theoretical studies are required to include this charge patchiness in the model of electrostatic complexation of PEs with oppositely charged objects. Moreover, in order to clarify the appearance of PE-induced bridging attraction, the influence of the length of a PE and its charge density on the properties of the (onset of) aggregation process and the structure of the resulting coacervates can be studied in experiments.

IV. SUMMARY

We have studied the adsorption of polyelectrolytes onto oppositely charge spheres. In the limit of strong adsorption, we have solved the linearized Poisson-Boltzmann equation for a particular charge pattern of the adsorbed PE. In the limit of weak adsorption, we have determined the critical adsorption temperature and the critical sphere charge density using the Edwards equation for polymer conformations. In both cases, we do not find an overcharging of the complexes as often predicted in the literature, particularly for strong PE adsorption. Our general procedure for the calculation of the electrostatic potential and energy in the strong adsorption limit allows us to calculate these quantities for a wide spectrum of charge distributions.

The solution of the Edwards equation for small sphere radii and weak adsorption strengths yields a dependence of the critical surface charge density on the Debye screening length, which is quite different from that for the planar geometry. The exponent of the κ dependence is close to that determined experimentally. Since in experiments typically the sphere radius is on the order of the PE persistence length, it is desirable to determine the critical quantities for adsorption of a *semiflexible* polymer. The dependence of critical adsorption characteristics on PE persistence length and screening length might differ from that found for adsorption of flexible PE chains studied in the present paper.

ACKNOWLEDGMENT

We thank P. Dubin for correspondence and comments.

[1] H. Schiessel, J. Phys.: Condens. Matter **15**, R699 (2003).
[2] K. Luger, A. M. Mäder, R. K. Richmond, D. F. Sangent, and T. J. Richmond, Nature (London) **389**, 251 (1997).
[3] R. R. Netz and J.-F. Joanny, Macromolecules **32**, 9026 (1999).
[4] F. von Goeler and M. Muthukumar, J. Chem. Phys. **100**, 7796 (1994).
[5] R. G. Winkler and A. G. Cherstvy, Phys. Rev. Lett. **96**, 066103 (2006).
[6] H. Schiessel, J. Rudnick, R. Bruinsma, and W. M. Gelbart, Europhys. Lett. **51**, 237 (2000).
[7] (a) T. T. Ngyuen and B. I. Shklovskii, J. Chem. Phys. **114**, 5905 (2001); (b) **115**, 7298 (2001); (c) Physica A **293**, 324 (2001).
[8] H. Schiessel, Macromolecules **36**, 3424 (2003).
[9] R. Messina, J. Chem. Phys. **117**, 11062 (2002).
[10] E. Zhulina, A. V. Dobrynin, and M. Rubinstein, Eur. Phys. J. E **5**, 41 (2001).
[11] A. G. Cherstvy and R. G. Winkler, J. Phys. Chem. B **109**, 2962 (2005).
[12] A. J. Spakowitz and Z.-G. Wang, Phys. Rev. Lett. **91**, 166102 (2003).
[13] R. J. Allen and P. B. Warren, Langmuir **20**, 1997 (2004).
[14] X. H. Feng, P. L. Dubin, H. W. Zhang, G. F. Kirton, P. Bahadur, and J. Parotte, Macromolecules **34**, 6373 (2001).
[15] A. B. Kayitmazer, E. Seyrek, P. L. Dubin, and B. A. Staggemeier, J.

Phys. Chem. B **107**, 8158 (2003).
[16] D. W. McQuigg, J. L. Kaplan, and P. L. Dubin, J. Phys. Chem. **96**, 1973 (1992).
[17] Y. Wang, P. L. Dubin, and H. Zhang, Langmuir **17**, 1670 (2001).
[18] H. Zhang, K. Ohbu, and P. L. Dubin, Langmuir **16**, 9082 (2000).
[19] A. B. Kayitmazer, D. Shaw, and P. L. Dubin, Macromolecules **38**, 5198 (2005).
[20] V. A. Kabanov, V. G. Sergeyev, O. A. Pyshkina, A. A. Zinchenko, A. B. Zezin, J. G. H. Joosten, J. Brackman, and K. Yoshikawa, Macromolecules **23**, 9587 (2000); I. Goessl, L. Shu, D. Schlueter, and J. P. Rabe, J. Am. Chem. Soc. **124**, 6860 (2002).
[21] A. A. Zinchenko, K. Yoshikawa, and D. Baigl, Phys. Rev. Lett. **95**, 228101 (2005); A. A. Zinchenko and A. Chen, J. Phys.: Condens. Matter **18**, R453 (2006).
[22] A. Laguecir, S. Stoll, G. Kirton, and P. L. Dubin, J. Phys. Chem. B **107**, 8056 (2003).
[23] T. Wallin and P. Linse, Langmuir **12**, 305 (1996); J. Phys. Chem. **100**, 17873 (1996).
[24] P. Chodanowski and S. J. Stoll, J. Chem. Phys. **115**, 4951 (2001); Macromolecules **34**, 2320 (2001); *ibid.* **35**, 9556 (2002).
[25] K.-K. Kunze and R. R. Netz, Phys. Rev. Lett. **85**, 4389 (2000).
[26] R. Podgornik, T. Åkesson, and B. Jönsson, J. Chem. Phys. **102**, 9423 (1995).
[27] A. Akinchina and P. Linse, Macromolecules **35**, 5183 (2002).
[28] H. Ohshima, Colloid Polym. Sci. **274**, 1176 (1996); *ibid.* **277**, 563 (1999).
[29] J. Stankovich and S. L. Carnie, J. Colloid Interface Sci. **216**, 329 (1999); Langmuir **12**, 1453 (1996).
[30] A. B. Glendinning and W. B. Russel, J. Colloid Interface Sci. **93**, 95 (1983).
[31] P.-G. de Gennes, Rep. Prog. Phys. **32**, 187 (1969).
[32] P.-G. de Gennes, *Scaling Concepts in Polymer Physics* (Cornell University Press, Ithaca, NY, 1979).
[33] R. R. Netz and D. Andelman, Phys. Rep. **380**, 1 (2003), and references therein.
[34] R. Varoqui, A. Johner, and A. Elaissari, J. Chem. Phys. **94**, 6873 (1991).
[35] R. Podgornik, J. Phys. Chem. **96**, 884 (1992).
[36] I. Borukhov, D. Andelman, and H. Orland, Europhys. Lett. **32**, 499 (1995).
[37] I. Borukhov, D. Andelman, and H. Orland, J. Phys. Chem. B **103**, 5042 (1999).
[38] O. V. Borisov, E. B. Zhulina, and T. M. Birshtein, J. Phys. II **4**, 913 (1994).
[39] I. Borukhov, D. Andelman, and H. Orland, Macromolecules **31**, 1665 (1998).
[40] R. R. Netz and J.-F. Joanny, Macromolecules **32**, 9013 (1999).
[41] X. Chatelllier and J.-F. Joanny, J. Phys. II **6**, 1669 (1996).
[42] A. Shafir, D. Andelman, and R. R. Netz, J. Chem. Phys. **119**, 2355 (2003).
[43] F. W. Wiegel, J. Phys. A **10**, 299 (1977).
[44] M. Muthukumar, J. Chem. Phys. **86**, 7230 (1987).
[45] T. T. Ngyuen, A. Yu. Grosberg, and B. I. Shklovskii, J. Chem. Phys. **113**, 1110 (2000).
[46] P. Haronska, T. A. Vilgis, R. Grottenmüller, and M. Schmidt, Macromol. Theory Simul. **7**, 241 (1998).
[47] M. Castelnovo and J.-F. Joanny, Eur. Phys. J. E **6**, 377 (2001).
[48] X. Chatellier and J.-F. Joanny, Eur. Phys. J. E **1**, 9 (2000).
[49] M. Elis, C. Y. Kong, and M. Muthukumar, J. Chem. Phys. **112**, 8723 (2000).
[50] A. G. Cherstvy and R. G. Winkler, J. Chem. Phys. **120**, 9394 (2004).
[51] Note that we solved the Poisson-Boltzmann equation outside of the sphere only. A different/low dielectric permittivity inside the sphere can affect the PE adsorption: the image forces can diminish the amount of adsorbed PE. Such situation is more relevant for DNA adsorption on a low-dielectric histone core in nucleosomes, but calculations become more cumbersome due to the dielectric discontinuity [see, for example, N. Hoffmann, C. N. Likos, and J.-P. Hansen, Mol. Phys. **102**, 857 (2004)].
[52] For the wrapping scenario of Fig. 1(b), the charge density for the spiral, which forms N_s full turns on the sphere surface and compensates fraction θ of the sphere charge, is $\sigma(\varphi,\vartheta)=\pi\sigma\theta N_s^{-1}\Sigma_{m=0}^{N_s-1}\delta(\vartheta-(2\pi m+\varphi)/(2N_s))$. Then $C_{lm}=-4\pi\varepsilon^{-1}k_l^{-1}\sigma\theta N_s^{-1}\Sigma_{m=0}^{N_s-1}(-1)^m\int_0^{2\pi}d\varphi\,\sin[(\varphi+2\pi m)/2N_s]Y_{l,-m}(\varphi,(\varphi+2\pi m)/(2N_s))\equiv-4\pi\varepsilon^{-1}k_l^{-1}P_{lm}$ and the electrostatic energy of the spiral is $E=-2\pi a^2\varepsilon^{-1}\Sigma_{l=0}^{\infty}\Sigma_{m=-l}^{l}(-1)^m P_{lm}P_{l,-m}k_l^{-1}K_{l+1/2}(\kappa a)/\sqrt{\kappa a}$.
[53] I. S. Gradshtein and I. M. Ryzhik, *Table of Integrals, Series and Products* (Verlag Harri Deutsch, Frankfurt, 1981), Vol. 2, Eq. 7.126.2.
[54] T. J. Odijk, J. Polym. Sci., Polym. Phys. Ed. **15**, 477 (1977); J. Skolnick and M. Fixman, Macromolecules **10**, 944 (1977).
[55] R. P. Mondescu and M. Muthukumar, Phys. Rev. E **57**, 4411 (1998).
[56] T. D. Yager, C. T. McMurray, and K. E. van Holde, Biochemistry **28**, 2271 (1989).
[57] I. Koltover, K. Wager, and S. R. Safinya, Proc. Natl. Acad. Sci. U.S.A. **97**, 14046 (2000).
[58] D. C. Rau and V. A. Parsegian, Biophys. J. **61**, 246 (1992); **61**, 260 (1992).
[59] A. G. Cherstvy, A. A. Kornyshev, and S. Leikin, J. Phys. Chem. B **106**, 13362 (2002); **108**, 6508 (2004); A. G. Cherstvy and A. A. Kornyshev, *ibid.* **109**, 13024 (2005); A. G. Cherstvy, J. Phys.: Condens. Matter **17**, 1363 (2005).
[60] M. de Frutos, E. Raspaud, A. Leforestier, and F. Livolant, Biophys. J. **81**, 1127 (2001); E. Raspaud, I. Chaperon, A. Leforestier, and F. Livolant, *ibid.* **77**, 1547 (1999).
[61] A. G. Cherstvy and R. Everaers (unpublished).
[62] A. A. Kornyshev and S. Leikin, J. Chem. Phys. **107**, 3656 (1997); Phys. Rev. Lett. **82**, 4138 (1999).
[63] H. Borourjerdi and R. R. Netz, Europhys. Lett. **64**, 413 (2003).
[64] S. Mangenot, A. Leforestier, P. Vachette, D. Durand, and F. Livolant, Biophys. J. **82**, 345 (2002).
[65] A. Katchalsky, O. Künzle, and W. Kuhn, J. Polym. Sci. **3**, 283 (1950); S. Lifson and A. Katchalsky, *ibid.* **11**, 409 (1953).
[66] C. S. Lam and Y. P. Varshni, Phys. Rev. A **4**, 1875 (1971).
[67] P. M. Morse and H. Feshbach, *Methods of Theoretical Physics* (McGraw-Hill, NY, 1953).
[68] G. S. Manning, Q. Rev. Biophys. **11**, 179 (1978).
[69] J.-L. Barrat and J.-F. Joanny, Adv. Chem. Phys. **94**, 1 (1996).
[70] M. Ullner, J. Phys. Chem. B **107**, 8097 (2003).
[71] T. Hofmann, R. G. Winkler, and P. Reineker, J. Chem. Phys. **118**, 6624 (2003).
[72] W. F. Reed, S. Ghosh, G. Medjahdi, and J. Francois, Macromolecules **24**, 6189 (1991).
[73] R. Everaers, A. Milchev, and V. Yamakov, Eur. Phys. J. E **8**, 3 (2002).
[74] K. W. Mattison, P. L. Dubin, and I. J. Brittain, J. Phys. Chem. B **102**, 3820 (1998).
[75] E. Seyrek, P. L. Dubin, C. Tribet, and E. A. Gamble, Biomacromolecules **4**, 273 (2003).
[76] C. L. Cooper, A. Goulding, A. B. Kayitmazer, S. Ulrich, S. Stoll, S. Turksen, S. Yusa, A. Kumar, and P. L. Dubin, Biomacromolecules **7**, 1025 (2006).